Domain organization of XAF1 and the identification and characterization of $XIAP^{RING}$-binding domain of XAF1

Man Kit Tse,[1,2] Chi Kong Cho,[1,2] Wai Fung Wong,[2] Bing Zou,[3] Sin Kam Hui,[2] Benjamin Chun Yu Wong,[3] and Kong Hung Sze[1,2]*

[1]Department of Microbiology and State Key Laboratory for Emerging Infectious Diseases, University of Hong Kong, Hong Kong SAR, People's Republic of China

[2]Department of Chemistry and Open Laboratory of Chemical Biology of the Institute of Molecular Technology for Drug Discovery and Synthesis, The University of Hong Kong, Hong Kong SAR, People's Republic of China

[3]Department of Medicine, University of Hong Kong, Hong Kong SAR, People's Republic of China

Received 21 May 2012; Revised 5 July 2012; Accepted 10 July 2012
DOI: 10.1002/pro.2126
Published online 18 July 2012 proteinscience.org

Abstract: X-linked inhibitor of apoptosis protein (XIAP)-associated factor 1 (XAF1) has been implicated as a novel tumor suppressor, which was proposed to exert pro-apoptotic effect by antagonizing the anticaspase activity of XIAP. Here, we delineated the domain architecture of XAF1 by applying limited proteolysis and peptide mass fingerprinting analysis. Our results indicated that XAF1 has a distinct domain organization, with a highly compact N-terminal domain ($XAF1^{NTD}$) followed by a middle domain ($XAF1^{MD}$), a 42-residue unstructured linker and a C-terminal domain ($XAF1^{CTD}$). The search of XIAP binding region within XAF1 revealed that a modest affinity $XIAP^{RING}$ binding site (dissociation constant, K_d, ~18 μM) is located at the C-terminal portion of XAF1. This C-terminal region, embracing $XAF1^{CTD}$ and a flexible tail at C-terminus (residue Thr251-Ser301), is functionally identified as $XIAP^{RING}$-binding domain of XAF1 ($XAF1^{RBD}$) in the present study. We have also mapped the interaction sites for $XAF1^{RBD}$ on $XIAP^{RING}$ by using NMR spectroscopy. By applying *in vitro* ubiquitination assay, we observed that $XAF1^{RBD}$/XIAP interaction is essential for the ubiquitination of GST-$XAF1^{RBD}$ fusion protein. In addition, the C-terminal XAF1 fragment harboring $XAF1^{RBD}$ was found to be substantially ubiquitinated by $XIAP^{RING}$. Base on these observations, we speculate a possible role of $XAF1^{RBD}$ in targeting XAF1 for XIAP-mediated ubiquitination.

Keywords: XAF1; XIAP; RING; ubiquitination; limited proteolysis; domain organization; apoptosis; protein-protein interaction; NMR spectroscopy

Statement

This work describes the systematic delineation of the domain architecture of XIAP-associated factor 1 (XAF1), which is a novel tumor suppressor and known to be a negative regulator of XIAP. We have also identified and characterized the interacting domains between XAF1 and XIAP by using GST pull-down assay, NMR spectroscopy, isothermal titration calorimetry, and *in vitro* ubiquitination assay. Based on these results, we proposed the possible roles of XAF1 in $XIAP^{RING}$-mediated ubiquitination and apoptosis.

Additional Supporting Information may be found in the online version of this article.

Grant sponsor: Research Grants Council of Hong Kong; Grant numbers: GRF 7755/08M and GRF 7765/09M; Grant sponsor: Special Equipment Grant from the University Grants Committee of Hong Kong SAR; Grant number: SEG/CUHK09.

*Correspondence to: Kong Hung Sze, Department of Microbiology and State Key Laboratory for Emerging Infectious Diseases, University of Hong Kong, Pokfulam Road, Hong Kong SAR, People's Republic of China. E-mail: khsze@hku.hk

Introduction

X-linked inhibitor of apoptosis protein (XIAP)-associated factor 1 (XAF1) is a 34 kDa pro-apoptotic zinc-finger rich protein, which has been implicated as a putative tumor suppressor.[1] The *xaf1* is an interferon (INF)-stimulated gene, and XAF1 is ubiquitously expressed in normal adult and fetal tissue. However, XAF1 mRNA expression is epigenetically down-regulated in various cancer cell lines by promoter hypermethylation.[2–4] Although the precise epigenetic regulating mechanisms remain largely undetermined, the restoring of XAF1 level in the tumor, either by epigenetic therapy or application of recombinant protein, represents a promising novel therapeutic approach in treatment of cancer.

At present, the exact mechanisms of XAF1 in affecting apoptosis remain unclear. Initially, it was proposed that XAF1 exerted its pro-apoptotic effect by directly antagonizing the anticaspase activity of XIAP, and triggering the nuclear sequestration of XIAP.[1] Subsequent studies demonstrated that XAF1 played multiple roles in apoptosis, such as induction of Bax expression, activation of mitochondrial pathway, and degradation of XIAP.[5] Although the apoptotic significances of XIAP-XAF1 interaction remain to be elucidated, the pro-apoptotic mechanisms of XAF1 are clearly more versatile than previously expected.

The current knowledge of the domain architecture and modular function of XAF1 is putative in nature. It is derived chiefly from multiple sequence alignment[1,2] and the identification studies of truncated splice variants of XAF1.[6,7] As a leading member of the IAP family of proteins, XIAP has been well characterized and extensively studied. XIAP has been shown to consist of three baculoviral IAP repeat (BIR) domains ($XIAP^{BIR1-3}$),[8] an evolutionarily conserved ubiquitin-associated domain ($XIAP^{UBA}$)[9] and a RING-finger domain ($XIAP^{RING}$) conferring ubiquitin protein ligase (E3) activity.[10] However, the molecular determinants involved in XIAP-XAF1 interaction remains undetermined.

In this report, limited proteolysis has been applied to identify three distinct domains in XAF1. Subsequently, nuclear magnetic resonance (NMR) spectroscopy, isothermal titration calorimetry (ITC), and GST pull-down experiments have been used to locate the $XIAP^{RING}$-binding domain in XAF1 ($XAF1^{RBD}$), which has been found to serve as the sole molecular determinant to mediate XAF1's interaction with XIAP. In addition, we have used NMR chemical shift perturbation (CSP) to map the XAF1 binding site on $XIAP^{RING}$. Unexpectedly, we observed that a C-terminal fragment of XAF1 harboring the $XAF1^{RBD}$ is a target for $XIAP^{RING}$-mediated ubiquitination. Based on these results, we will discuss the possible roles of $XAF1^{RBD}$ in $XIAP^{RING}$-mediated ubiquitination and apoptosis.

Results

Domain organization of human XAF1

The domain architecture of full-length human XAF1 (residues Met1-Ser301, Swiss-Prot entry Q6GPH4) has not been clearly defined. Previous protein sequence analysis on XAF1 predicted that it contained seven zinc finger (Znf) motifs[1] [Fig. 1(C)]. The N-terminal region, embracing the first five Znf motifs, is a homologous counterpart (~41% identity) of the TRAF-typed zinc finger domain in human FLN29 protein.[1]

To investigate the domain organization of XAF1 experimentally, we performed limited proteolysis using trypsin digestion enzyme. Proteolytic stable products were separated by gel electrophoresis, followed by in-gel digestion and peptide mass fingerprinting (PMF) using matrix-assisted laser desorption/ionization time of flight mass spectroscopy (MALDI-TOF MS) [Fig. 1(A) and Supporting Information Table S1). Partially purified GST-XAF1 protein, when subjected to proteolytic treatment with trypsin, gave two intense bands (F0 and F1) above the 14 kDa marker position on a Coomassie-stained SDS-PAGE [Fig. 1(A), top panel]. A database search and manual verification of PMF data of F0 and F1 showed that the peptide bonds of the arginine residue at the linker region (LVPRGSPEF) of GST-XAF1 expression construct and at sequence position 143 were cleaved, resulting in the release of the GST moiety (F0) and a trypsin-resistant XAF1 fragment (F1, residues Met1-Arg143), respectively [Fig. 1(B)].

In order to provide further support for the existence of a structural domain within this region of residues Met1-Arg143, we performed circular dichroism (CD) and two-dimensional ^{1}H-^{15}N Heteronuclear Single Quantum Coherence (HSQC) NMR spectroscopy on a purified XAF1 fragment corresponding to this region. The far-UV CD spectrum showed two negative bands of different magnitudes at around 207 and 222 nm, characteristic of α-helical and β-sheets structures [Fig. 2(A), top panel]. The result indicated that this XAF1 fragment exhibits a well-defined secondary structure. The NMR data also supported that it has a well-folded protein core. The amide cross-peaks of the ^{1}H-^{15}N HSQC spectrum were well-dispersed [Fig. 2(B)]. Furthermore, the CD-monitored denaturation curves were sigmoidal in shape, indicating the denaturation is a cooperative process, thereby strongly suggesting the existence of a compact domain in this N-terminal region of XAF1 [Fig. 2(A), bottom panel]. Therefore, residues Met1-Arg143 of XAF1 is defined as an N-terminal domain, $XAF1^{NTD}$, in the present study.

To explore the domain architecture of C-terminal region of XAF1, we generated a His_6-tagged XAF1 fragment (His_6-$XAF1_{106–301}$, residues Gly106-Ser301) and subjected it to limited proteolysis using

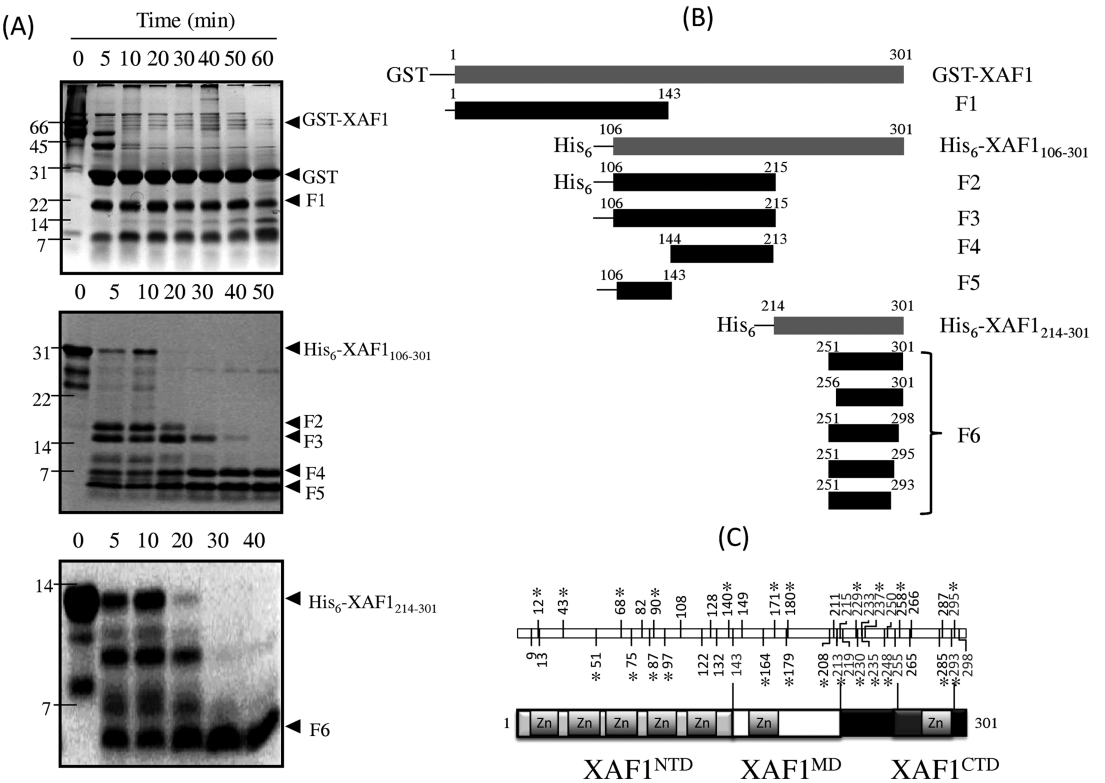

Figure 1. Domain organization of XAF1. (A) Time-course of limited proteolysis of XAF1 and its fragment. GST-XAF1 (top panel), His_6-$XAF1_{106–301}$ (middle panel) and His_6-$XAF1_{214–301}$(bottom panel) was subjected to proteolysis by trypsin and visualized by Coomassie blue stained SDS-PAGE, respectively. Major proteolytic fragments marked with black arrowheads were identified by MALDI-TOF MS and are shown schematically in (B). Endpoint numbering follows full-length XAF1 numbering scheme. The mass spectrometric data used to identify fragment endpoints is available as Supporting Information. (C) (Top panel) Summary of the trypsin-sensitive (light gray) and trypsin-resistant (black) cleavage sites of XAF1 identified in the present study. Asterisk indicates lysine residue. (Bottom panel) Schematic domain organization of full-length XAF1. Structural domain regions are color coded: Light gray, $XAF1^{NTD}$; white: $XAF1^{MD}$; dark gray: $XAF1^{CTD}$. Flexible regions are colored as black. ZN donates zinc finger motif.

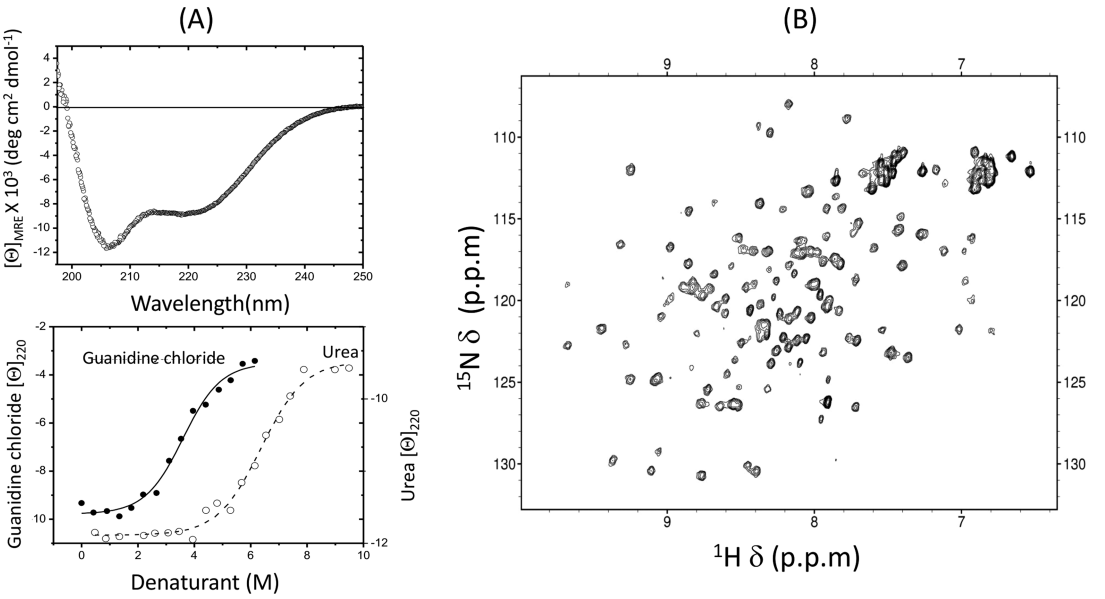

Figure 2. Structural characterization of $XAF1^{NTD}$. (A) (Top panel) The far-UV CD spectrum of $XAF1^{NTD}$. (Bottom panel) Urea-induced (open circle) and guanidine chloride-induced (close circle) equilibrium denaturation curves measured as ellipticity of $XAF1^{NTD}$ at 222 nm. (B) ^1H-^{15}N HSQC spectrum of $XAF1^{NTD}$.

trypsin enzyme digestion. Proteolysis of His_6-$XAF1_{106-301}$ gave rise to two moderately stable fragments in gel bands F2 and F3 immediately after the addition of protease. Prolonged incubation with trypsin yielded two proteolytic stable fragments in bands F4 and F5 [Fig. 1(A), middle panel]. The PMF analysis along with the mass measurements (Supporting Information Tables S1 and S2) indicated that bands F2 and F3 correspond to a fragment encompassing the same amino acid sequence (residues Gly106-Arg215), except that F3 lacks the N-terminal His_6-tag [Fig. 1(B)]. The XAF1 fragment in band F3 was further cleaved at the residues Arg143 and Lys213, resulting in peptide bands F4 (residues Ile144-Lys213) and F5 (residues Gly106-Arg143, containing the C-terminus Znf motif of $XAF1^{NTD}$), respectively [Fig. 1(B), middle panel]. These results established that residues Ile144-Lys213 represent a newly identified middle domain ($XAF1^{MD}$), which is consecutively connected to the $XAF1^{NTD}$ at residue Arg143.

For the remaining C-terminal portion of the XAF1, we have conducted similar digestion studies on a purified His_6-tagged XAF1 fragment, His_6-$XAF1_{214-301}$, corresponding to residues Thr214-Ser301. A third protected fragment corresponding to gel band F6 [Fig. 1(A), bottom panel] was located at the C-terminal end of the XAF1 protein. According to the MS data, band F6 contained a mixture of peptides, sharing a common segment, residues Gly256-Lys293, at the interior region of His_6-$XAF1_{214–301}$ [Fig. 1(B), Supporting Information Table S2). This XAF1 segment is denoted as C-terminal domain ($XAF1^{CTD}$), which is separated from the $XAF1^{MD}$ by a 42-residue spanning linker (residues Thr214-Arg255). Lysine and arginine residues within this linker were all susceptible to proteolysis, suggesting that the linker is structurally disordered. The $XAF1^{CTD}$ is followed by a short C-terminal flexible tail covering residues Leu294-Ser301.

Based on these limited proteolysis data, we concluded that human XAF1 possesses distinct domain architecture with well-defined domain boundaries [Fig. 1(C)]: Met1-Arg143 ($XAF1^{NTD}$), Ile144-Lys213 ($XAF1^{MD}$), and Gly256-Lys293 ($XAF1^{CTD}$). A spanning unstructured 42-residue linker connects the $XAF1^{MD}$ and $XAF1^{CTD}$, which was readily accessible to trypsin digestion. Residues within the $XAF1^{NTD}$ were predicted to form a TRAF-like zinc finger domain.[1] Our CD and NMR data provided further support for the existence of a compact structural moiety within this N-terminal part of human XAF1.

Identification of $XIAP^{RING}$ binding domain in XAF1

In an attempt to identify the molecular determinant(s) of XAF1 that mediates the interaction with XIAP, *in vitro* GST pull-down assay was conducted to evaluate the interaction of GST-XAF1 with a panel of GB1-His_6 tagged full-length XIAP (GB1-His_6-XIAP) and its domain fragments. A band at the molecular mass of GB1-His_6-XIAP, which immunereacted with anti-XIAP antibody, was detected with GST-XAF1 but not with GST alone [Fig. 3(A)]. As shown in Figure 3(A), all $XIAP^{RING}$-bearing fragments, as well as the $XIAP^{RING}$ alone, showed interactions with GST-XAF1. Our result is in agreement with previous report that XAF1 directly interacted with all RING-bearing IAPs.[11] In a subsequent series of pull-down assays using various truncated GST-XAF1 fragments as baits, we found that XAF1 was solely associating with $XIAP^{RING}$ via its C-terminal portion (residues Thr214-Ser301), including the $XAF1^{CTD}$ [Fig. 3(B), lane 6].

To further refine the $XIAP^{RING}$-binding region of XAF1 within residues Thr214-Ser301, we performed ^1H-^{15}N HSQC titration experiments of ^{15}N-His_6-$XAF1_{214–301}$ with unlabeled $XIAP^{RING}$. Upon $XIAP^{RING}$ binding, various resonances of the ^{15}N-His_6-$XAF1_{214–301}$ disappeared, suggesting that this interaction falls into the intermediate exchange regime on the NMR chemical shift time scale (Supporting Information Fig. S1). At intermediate exchange, NMR resonances of the residues involved in intermolecular interaction will be broadened, leading to the weakening and/or disappearing of their signals.[12] For a quantitative evaluation, the peak intensity ratios between free and bound ^{15}N-His_6-$XAF1_{214-301}$ were evaluated using a molar ratio of 1:1 sample (Supporting Information Fig. S1 and Fig. 3C). A majority of peaks corresponding to the backbone amide signals within residues Ala259-Ser301 disappeared. This suggested that the segment corresponding to residues Ala259-Ser301 forms the binding region of $XIAP^{RING}$. Therefore, we have designated the region covering residues Thr251-Ser301, which includes the $XAF1^{CTD}$ and the flexible C-terminus tail of XAF1, as $XIAP^{RING}$-binding domain ($XAF1^{RBD}$) in the present study.

To quantify the affinity between $XAF1^{RBD}$ and $XIAP^{RING}$, isothermal titration calorimetry (ITC) experiment was performed using purified $XAF1^{RBD}$ and $XIAP^{RING}$ [Fig. 3(D), left panel]. The dissociation constant (K_d) was determined to be 18.5 ± 2 μM. The binding stoichiometry was measured to be around 0.9. This result showed that $XAF1^{RBD}$ contains a single moderate-affinity binding site for the $XIAP^{RING}$. The C-terminal deletion mutant of $XAF1^{RBD}$, $XAF1^{RBD}\Delta C$ (residues Thr251-Ser292), showed no detectable binding by ITC [Fig. 3(D), right panel]. This result suggested that the flexible C-terminus tail of XAF1 (residues Lys293-Ser301) is essential for interaction with $XIAP^{RING}$. The binding affinity observed between $XAF1^{RBD}$ and $XIAP^{RING}$ is highly comparable with those reported for the association of ubiquitin conjugating enzyme UbcH5B (E2) with the RING domain of cIAP-2 ($cIAP\text{-}2^{RING}$)

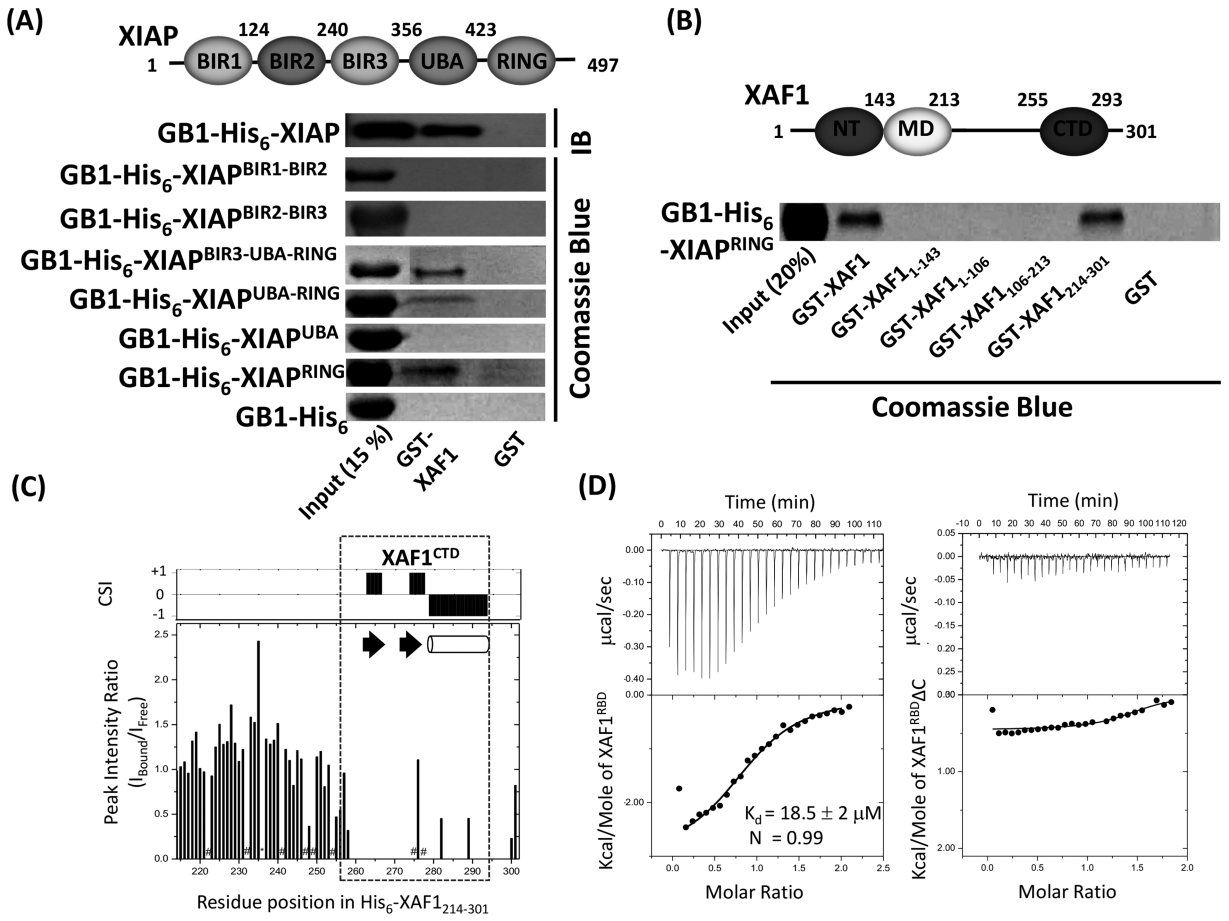

Figure 3. Identification of XAF1^{RBD} in XAF1. (A) (Top panel) Schematic diagram showing the domain organization of XIAP. The domain boundaries of the protein constructs, used in this study, are indicated. (Bottom panel) A GST pull-down assay showing that the GST-tagged XAF1 specifically binds to XIAP^{RING}. IB: Immunoblot analysis (anti-XIAP antibody). (B) (Top panel) Schematic representation of the domain organization of XAF1 with the domain boundaries identified in this study. A GST pull-down assay indicates that the C-terminal region of XAF1 binds to XIAP^{RING}. (C) The calculated peak intensity ratio of the C-terminal XAF1 fragment (His$_6$-XAF1$_{214–301}$) after the addition of XIAP^{RING}. Chemical shift index (CSI) plot is indicated on top. Proline and the residues that exhibited peak broadening are marked by asterisks and numbered sign, respectively. The region of XAF1^{CTD} is indicated by dashed-line rectangle. (D) ITC titrations of XIAP^{RING} with XAF1^{RBD} (left panel) or XAF1^{RBD}ΔC (right panel). Deletion of C-terminal flexible tail of XAF1 abolished the binding.

(K_d = 19–43 µ*M*, as determined by ITC) and with XIAP^{RING} (as determined by GST pull-down experiment).[13]

Mapping of XAF1^{RBD}-binding surface on XIAP^{RING}

To localize the XAF1^{RBD} binding site on XIAP^{RING}, NMR chemical shift perturbation (CSP) experiments were performed by monitoring the ^{1}H-^{15}N TROSY-HSQC spectrum of ^{15}N-XIAP^{RING} upon the addition of increasing amounts of unlabeled XAF1^{RBD}. During the course of titration, we observed both significant chemical shift perturbations and cross-peak intensity attenuations in certain backbone amide resonances, indicating that these residues are likely located at or close to the binding interface. Mapping the locations of these significantly changed residues onto the structure of XIAP^{RING} (PDB ID: 2ECG) revealed that residues in the stretches of Lys451-Met454 (α1-β1 loop) and Glu476-Thr489 (C-terminal portion of α2 helix and α2-β3 loop) contributed to a specific XAF1^{RBD}-binding pocket on XIAP^{RING} [Supporting Information Fig. S2 and Fig. 4(A,B)].

The RING domain is known to function as an E3 ligase, which confers specificity to ubiquitination by serving as a scaffold to recruit ubiquitin-charged E2 (Ub-E2).[14,15] However, the molecular details of how the RING domain, in the ternary complex, mediating the transfer of ubiquitin from E2 to target substrate is still largely unknown.[15] Previous studies demonstrated that the RING domains of IAP family members associated with overlapping but partially distinct subset of E2s.[16] XIAP and cIAP-2 could interact with UbcH7 and all of the UbcH5 family members (i.e., UbcH5A-C). Recently, an X-ray crystallographic study revealed that interaction between cIAP-2^{RING} and UbcH5B involves the cIAP-2^{RING} residues in the helix α1, α1-β1 loop, and α2-β3

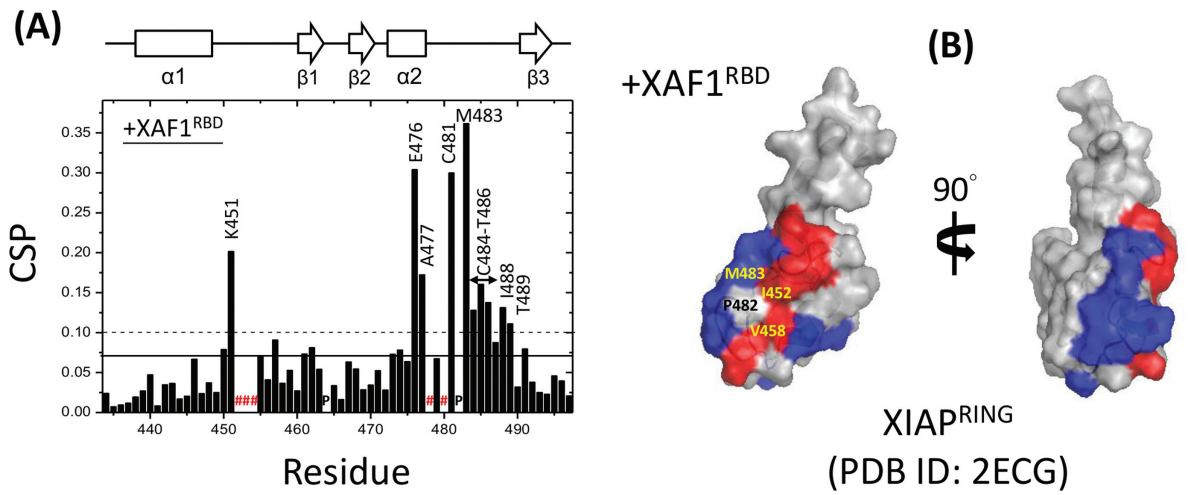

Figure 4. Mapping of XAF1^{RBD} binding interface on XIAP^{RING}. (A) The residue-wise chemical shift perturbation (CSP) in XIAP^{RING} upon the addition of XAF1^{RBD}. The average (solid line) and the average plus one standard deviation (SD) (dotted line) of CSP values are indicated. Residues that exhibited peak broadening are marked by red numbered sign. Prolines are marked by "P." The secondary structures along the sequence are marked at the top. (B) Surface map of significantly perturbed residues in XIAP^{RING} upon XAF1^{RBD} binding. Residues with a CSP value higher than one SD above the average was considered as significantly perturbed and are colored blue. Peaks broadening residues are colored red.

loop.[13] It is intriguing to note that the XIAP^{RING} residues perturbed upon XAF1^{RBD} binding are located near to the primary sequence positions [Met483, Ile452, and Val458, Fig. 4(B)] where homologous residues of cIAP-2^{RING} are involved in the interaction with E2.[13] Therefore, XAF1 may act as either a competitive inhibitor of XIAP^{RING}-dependent ubiquitination cascade by displacing E2 from XIAP^{RING}, or simply as a substrate for ubiquitination.

GST-XAF1^{RBD} is a target for ubiquitination through interaction with XIAP^{RING}

Based on the present ITC measurement and previously reported studies,[13] XIAP^{RING} possesses a comparable affinity for binding of XAF1^{RBD} and UbcH5b. To test whether XAF1^{RBD} could act as a competitive inhibitor of XIAP^{RING}-dependent ubiquitination cascade by displacing E2 from XIAP^{RING}, *in vitro* E3 ligase activities of XIAP^{RING} in the presence and absence of XAF1^{RBD} were measured. The *in vitro* E3 ligase activity of XIAP^{RING}, as shown by its autoubiquitination, remained unchanged even in the presence of 10-fold molar excess of XAF1^{RBD}. This result implied that XAF1^{RBD} cannot effectively displace E2 and to inhibit the ligase activity of XIAP^{RING} (Supporting Information Fig. S3).

Unexpectedly, ubiquitinated GST-XAF1^{RBD} was detected by using anti-GST antibody during western blotting of a standard *in vitro* ubiquitination assay using GST-XAF1^{RBD} as the substrate and GB1-His$_6$-XIAP as the E3 ligase. It should be noted that the ubiquitination could also be observed even using GST-XAF1^{RBD} (NO-K) [Fig. 5(B)], which is a GST-XAF1^{RBD} mutant where all lysine residues in the XAF1^{RBD} have been replaced by arginine (K258R, K285R, K293R, K295R) thereby impeding ubiquitin conjugation on the XAF1^{RBD} moiety. In contrast, when GST alone or GST-tagged XAF1$^{RBD}\Delta$C was included in the ubiquitination assay, ubiquitinated adducts of GST or GST-XAF1$^{RBD}\Delta$C were not observed [Fig. 5(B)]. Given that the XIAP binding affinity for the GST-XAF1^{RBD} (NO-K) is not significantly different from that of the wild type GST-XAF1^{RBD} [Fig. 5(A)], our result indicated that XAF1^{RBD}/XIAP interaction induces the ubiquitination of GST moiety in the GST-XAF1^{RBD} via the E3 ligase activity of XIAP^{RING} in GB1-His$_6$-XIAP. Disruption of the interaction between XAF1^{RBD} and XIAP^{RING} by deleting the C-terminal tail of XAF1^{RBD} will totally abolish this effect [Figs. 3(D) and 5(A) lane 4 and 5(B) lane 5). These results suggested that XAF1^{RBD} may function as a promoter of XIAP^{RING}-mediated ubiquitination.

The C-terminal XAF1 fragment is ubiquitinated by XIAP^{RING}

We speculate that the interaction between XIAP^{RING} and XAF1^{RBD} at the C-terminal end of full-length XAF1 may somehow induce the XIAP^{RING}-mediated ubiquitination of the N-terminal portion of a XAF1 fragment containing the XAF1^{RBD}. Indeed, the N-terminal truncated XAF1 fragment (His$_6$-XAF1$_{214–301}$), harboring the XAF1^{RBD} and the unstructured XAF1 linker, was found to be significantly ubiquitinated by XIAP^{RING}. On the other hand, the C-terminal truncation XAF1 mutant (residues Met1-Lys213, XAF1^{NTD-MD}), composed of XAF1^{NTD} and XAF1^{MD} only, showed no ubiquitination by XIAP^{RING} [Fig. 5(C)].

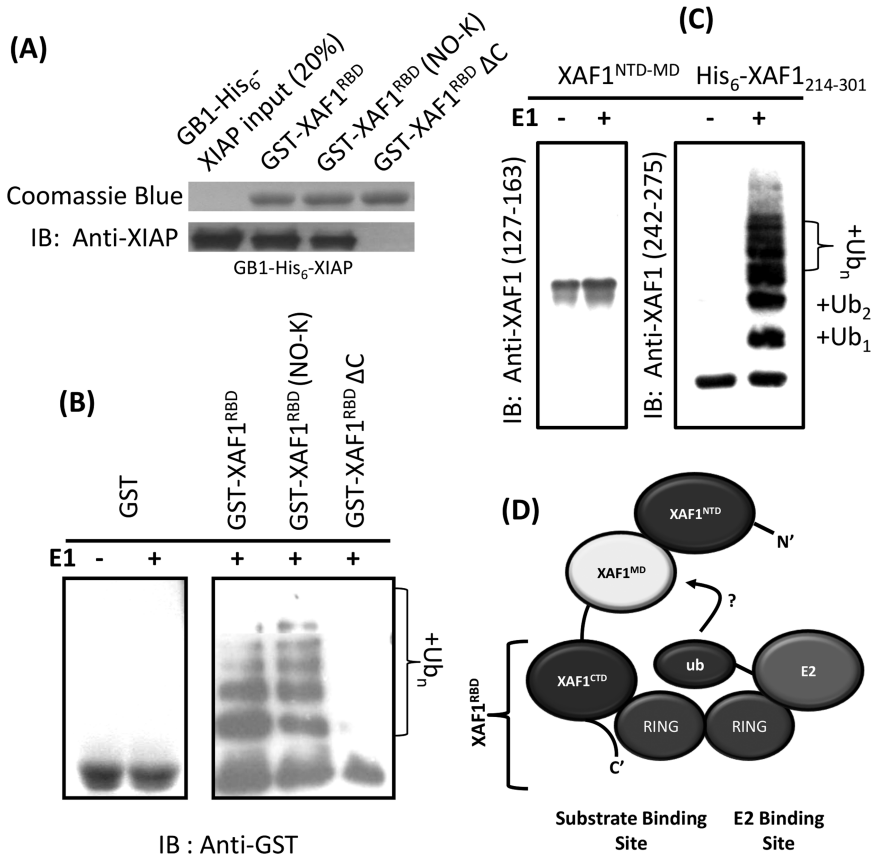

Figure 5. Protein harboring XAF1^{RBD} is a substrate of XIAP^{RING}-mediated ubiquitination. (A) GST pull-down assays show that GB1-Hi$_{s6}$-XIAP interacts with GST- XAF1^{RBD} and GST-XAF1^{RBD} (NO-K) but not with GST-XAF1^{RBD}ΔC. (B) In *vitro* XIAP-mediated ubiquitination assay of GST-XAF1^{RBD} and its mutant. Binding of XAF^{RBD} and XIAP induces ubiquitination of GST moiety at N-terminal. (C) *In vitro* XIAP^{RING}-mediated ubiquitination assay of XAF1 fragments. XAF1 fragment containing XAF1^{RBD} is ubiquitinated. IB: Immunoblot analysis (anti-GST antibody for panel B, anti-XAF1 (127–163), and anti-XAF1 (242–275) antibodies for panel C). (D) Proposed mechanism of XIAP^{RING} for its dual role in XAF1 recognition and ubiquitination. The ubiquitin is transferred from E2-Ub to XAF1 in an unknown manner.

Discussion

XIAP-associated factor 1 (XAF1) is a 301-amino acids interferon (INF)-inducible pro-apoptotic protein. It is found to have extremely low level in numerous cancer cells,[2] thereby implicating XAF1 as a putative tumor suppressor.[1] The molecular mechanisms underlying the pro-apoptotic activity of XAF1 remain unclear. XAF1 was initially proposed to antagonize the anticaspase activity of XIAP by nuclear sequestration of XIAP-XAF1 complex.[1] It was later reported that XAF1 can translocate into mitochondria and activates the intrinsic pathway of apoptosis.[5]

The molecular determinant involved in XIAP-XAF1 interaction remains largely unknown except it has been reported that XAF1 can interact with all RING-bearing IAPs including XIAP.[11] Here, we have extended this interaction study with the identification of the XAF1^{RBD} domain responsible for the interaction with XIAP. We have accidentally discovered that this XAF1^{RBD} could induce the ubiquitination of the GST fusion tag at its N-terminal via its interaction with the RING domain of XIAP. Following up on this discovery, the C-terminal XAF1 fragment containing XAF1^{RBD} was found to be substantially ubiquitinated by XIAP^{RING} *in vitro*. It should be noted that the C-terminal region of XAF1 has been suggested to be crucial for its pro-apoptotic activity in the previous studies.[6,17] An artificially C-terminal truncated form of XAF1 (residues 1–178) has also been reported to act in a dominant negative manner, blocking the ability of INF-β to sensitize cell to TRAIL-induced apoptosis.[17] In addition, a previous study showed that the mRNA expression ratio of XAF1A (full-length) and XAF1C (splice variant contains only the XAF1^{NTD}) differs among cancer cell lines derived from a variety of tissue types.[6] Our results implied the possibility that the ubiquitination of putative tumor suppressor XAF1, presumably via association between XAF1^{RBD} and XIAP^{RING}, may be involved in regulating apoptosis.

The role of XIAP in the ubiquitin-mediated regulation of apoptosis is emerging.[10] XIAP^{RING} has been demonstrated to be required for the

ubiquitination and proteasomal degradation of several XIAP-associated apoptosis-related proteins, such as caspase-3[18] and direct inhibitor of apoptosis-binding protein with low pI (DIABLO).[19] In this sense, $XIAP^{RING}$ may also regulate the cellular level of XAF1 through the ubiquitin-proteasome pathway. In particular, it is known that the cellular expression ratio of XIAP and XAF1 could control the cell fate.[20,21] Furthermore, it is possible that XAF1 may act as a promoter of the XIAP-mediated ubiquitination. It should be noted that XIAP-mediated ubiquitination of XAF1 has been reported to be involved in the proteasomal degradation of a ternary complex of XAF1-XIAP-Survivin.[11] In this ternary complex, XAF1 may either be itself ubiquitinated or promote the XIAP-mediated ubiquitination of Survivin in the vicinity of XAF1-XIAP, in a manner similar to the ubiquitination of GST moiety in GST-$XAF1^{RBD}$ observed in the present work. Although the same study also demonstrated that XAF1 can associate with all RING-bearing IAPs,[11] we cannot exclude the possibility that ubiquitination of XAF1, mediated by the RING domain of XIAP or other IAPs, may serve nonproteasomal regulatory functions such as signal transduction[22,23] and intracellular trafficking among compartments and organelles.[24] It was reported that cIAP-1 and cIAP-2 can mediate K6-linked,[25] K11-linked,[26] and monoubiquitination[27] of substrates for nonproteasomal functions. In future experiments, it will be interesting to fully characterize the physiological ubiquitination function of XAF1 in apoptosis.

It has been reported that the RING domains in IAPs belong to the dimeric RING finger family.[28] By gel filtration analysis, the estimated molecular mass of purified $XIAP^{RING}$ protein, in the present study, was 15,512 Da, which is consistent with a dimeric form of $XIAP^{RING}$ (Supporting Information Fig. S4). During ubiquitination, the RING domain dimer serves as a scaffold to bind Ub-E2 and mediates the transfer of ubiquitin to the target substrate, which interacts with the substrate binding domain in conjunction with either protomer RING units.[15] To catalyze the ubiquitination, IAP protein possesses BIR domain for substrate recognition and capture.[28,29] Several XIAP-associated proteins, including DIABLO, caspase-3, and apoptosis-inducing factor (AIF),[30] contain a canonical IAP binding motif (IBM) which interacts with the IBM-interaction groove locating on the BIR domain of XIAP,[8] and thereby presumably enabling them to be ubiquitinated by the RING domain of XIAP.[29] Our result showed that XAF1 do not interact with any BIR domains of XIAP [Fig. 3(A)], which is consistent with the fact that XAF1 does not contain any IBM motif. Instead, the C-terminal XAF1 fragment (residues Thr214-Ser301) containing $XAF1^{RBD}$ could serve as an ubiquitination substrate of $XIAP^{RING}$ alone. The XAF1/XIAP interaction seems to be mediated primarily, if not solely, by the specific interaction between $XAF1^{RBD}$ and $XIAP^{RING}$. It should also be noted that although the $XAF1^{RBD}$-binding site on $XIAP^{RING}$ was shown to be overlapping partially with the regions required for UbcH5-binding, 10-fold molar excess of $XAF1^{RBD}$ was not able to inhibit the action of UbcH5b in the auto-ubiquitination experiment of GB1-His_6-$XIAP^{RING}$. Therefore, we speculate that both $XAF1^{RBD}$ and E2-Ub simultaneously bind to a $XIAP^{RING}$ dimer. One protomer RING unit serves as a substrate-recognition site to bind $XAF1^{RBD}$ while the binding of E2-Ub occurs at the second protomer RING unit. This will catalyze the formation of isopeptide bond between the ubiquitin and the lysine residue of the C-terminal XAF1 fragment anchoring on the complementary protomer [Fig. 5(D)]. Therefore, $XAF1^{RBD}$/$XIAP^{RING}$ interaction appears to be important for the substrate-recognition for XIAP-mediated ubiquintation. However, at present, we cannot discern whether $XAF1^{RBD}$ will promote ubiquintation on other XIAP-associated proteins, such as DIABLO, caspase-3, AIF, and Survivin. Further studies will be needed to fully characterize the functional role of $XAF1^{RBD}$ in the context of apoptosis regulation through XIAP-mediated ubiquitination.

Materials and Methods

Protein expression and purification

The genes encoding full-length human XIAP (Met1-S497) and its domain containing fragments (Met1-Glu240 ($XIAP^{BIR1-BIR2}$), Glu240-Thr356 ($XIAP^{BIR2-BIR3}$), Glu240-Ser497 ($XIAP^{BIR3-UBA-RING}$), Thr356-Ser497 ($XIAP^{UBA-RING}$), Thr356-Gln433 ($XIAP^{UBA}$), and Glu434-Ser497 ($XIAP^{RING}$)) were ligated into pGEX-4T-1 (GE-healthcare) and pGB1-HIS vectors. Likewise, the DNA sequences encoding the full-length human XAF1 (Met1-Ser301) and its fragments, (Met1-Gly106, Met1-Arg143($XAF1^{NTD}$), Met1-Lys213($XAF1^{NTD-MD}$), Gly106-S301, Gly106-Lys213, Thr214-Ser301, Thr251-Ser301($XAF1^{RBD}$), and Thr251-Ser292 ($XAF1^{RBD}\Delta C$)), were all subcloned into pGEX-4T-1, pET-H, and pGB1-HIS,[9] yielding fusion proteins with an N-terminal GST, His_6, and GB1-His_6 tags, respectively. $XAF1^{RBD}$ mutants were prepared by site-directed mutagenesis of the wild-type GST-tagged expression construct using a QuickChange Site-Directed Mutagenesis Kit (Stratagene). For recombinant protein expressions, the DNA constructs were transformed into *Escherichia coli* host BL21 (DE3) (Novagen). Unlabeled protein was prepared from cells grown in Luria-Bertani (LB) media supplemented with 50 μM $ZnSO_4$. Uniformly ^{15}N-labeled proteins were obtained from cells grown in M9 minimal media incorporating [U-^{15}N]-ammonium chloride (Cambridge Isotopes Laboratories, CIL) as the sole nitrogen source. The

expression and purification of His_6-, GB1-His_6-, and GST-tagged XAF1 and XIAP proteins were essentially the same as previously described.[9] Briefly, $XAF1^{NTD}$, $XAF1^{NTD\text{-}MD}$, $XAF1^{RBD}$, and $XIAP^{RING}$ protein domains were purified by GST affinity chromatograph, on column thrombin digestion at 25°C for 12 h, and gel filtration on a Superdex 75 prep grade column (GE healthcare). The His_6- and GST-tagged E2s (UbcH5A-C) were expressed and purified as previously described.[31] All protein samples were prepared in buffer HB (20 m*M* Tris-HCl, pH 7.4, 100 m*M* NaCl, 1 m*M* DTT).

Limited proteolysis and MALDI-TOF MS analysis

All proteins were concentrated to 1 mg/mL before limited proteolysis experiment. Limited proteolyses by trypsin (Fluka, TCPK-treated) were carried out at room temperature in a protein to protease ratio of 3000: 1. After the incubation has started, samples were collected at 0, 5, 10, 20, 30, 40, 50, and 60 min. PMSF (2 m*M*) was added to terminate the reaction. The samples were divided into two equal portions. One half of the sample was mixed with 3× Laemmli buffer, followed by SDS-PAGE electrophoresis and Coomassie blue gel staining. Gel bands were excised and submitted to the Research Genome Center core services at The University of Hong Kong for MALDI-TOF PMF (Supporting Information Table S1). Another half of the sample was treated with 0.1% TFA. Thereafter, molecular masses of the proteolytic products were analyzed by Voyager linear MALDI-TOF spectrometer (PerSeptive Biosystems) (Supporting Information Table S2).

Circular dichroism (CD) spectroscopy

All the far-UV (195–250 nm) CD spectra were recorded on a JASCO model 810 instrument at 25°C using 1 mm path-length sample cell. About 0.5 mg/mL of protein were prepared in buffer HB for the experiment. For the denaturant-induced unfolding, stock solutions of guanidine chloride (8*M*) and urea (9.8*M*) were added to 200 μL of 0.2 mg/mL protein at various concentrations (0–8*M*). The mixture was incubated at 25°C for at least 1 h before far-UV CD measurement.

In vitro *GST-pull down assay and ubiquitination assay*

Proteins used in GST pull-down assay were purified as described in the previous section. Purified GST or GST-tagged XAF1 fragments (200 μg each) were incubated with GB1-His_6-XIAP domains (100 μg each) at 4°C for 2 h in the presence of 0.1% BSA. The complex was immobilized on Glutathione-Sepharose 4B beads (GE Healthcare), followed by extensively washing in PBS. The bound materials were eluted with 3× Laemmli buffer and analyzed by SDS-PAGE followed by Coomassie Blue staining or ImmunoBlot (IB) analyses with an anti-XIAP antibody (Thermo Scientific).

For *in vitro* ubiquitination assay of GST-$XAF1^{RBD}$, substrates including GST, GST-$XAF1^{RBD}$, and mutated GST-$XAF1^{RBD}$ were incubated, respectively with Glutathione-Sepharose 4B resin, followed by extensive washing with buffer U (10 m*M* Tris-HCl, pH 7.4, 100 m*M* NaCl, 3 m*M* $MgCl_2$, 2 m*M* DTT, 5 m*M* ATP). The resin was then resuspended in 30 μL of a reaction mixture which is named buffer U, containing 50 ng human E1 (Boston Biochem), 0.4 μg human E2 UbcH5B (Boston Biochem), 100 μg ubiquitin (Boston Biochem), and 3 μg E3 (GB1-His_6-XIAP). Reactions were carried out at 30°C for 1 h. The resin was washed again by buffer U followed by boiling in 50 μL 1× Laemmli's buffer. Ubiquitinated GST-tagged proteins were separated on SDS-PAGE and detected by Anti-GST (Santa Cruz).

For ubiquitination assays of $XAF1^{NT\text{-}MD}$ and His_6-$XAF1_{214–301}$, 100 μg of substrate ($XAF1^{NT\text{-}MD}$ or His_6-$XAF1_{214–301}$) was contained in the above reaction mixture. Reactions were carried out at 37°C for 45 min, and terminated by boiling in 1× Laemmli's buffer. Ubiquitinated XAF1 proteins were separated on SDS-PAGE and detected by Anti-XAF1 (127–163) and Anti-XAF1 (215–301) (Santa Cruz), which specifically recognizes epitopes between residues 127–163 and 215–301 of XAF1, respectively.

Isothermal titration calorimetry

ITC experiments were performed with a VP-ITC instrument (MicroCal). Typically, 1 m*M* of $XAF1^{RBD}$ or $XAF1^{RBD}\Delta C$ was titrated into a 100 μ*M* solution of $XIAP^{RING}$. Experiments were carried out at 25°C in a buffer containing 10 m*M* HEPES, pH 7.4, 100 m*M* NaCl. The data were analyzed using Origin 7. The binding constant was obtained by fitting the thermogram into a one site binding model.

NMR spectroscopy and titration studies

NMR studies were performed at 298 K using a Bruker Advance 700 MHz NMR spectrometer equipped with a TCI cyroprobe. Data were acquired and processed using TopSpin 2.1 (Bruker) and SPARKY. All samples were buffer-exchanged into buffer BT (20 m*M* BisTris-HCl, pH 6.7, 150 m*M* NaCl, 5 m*M* d_{10}-DTT, 1 m*M* PMSF, 90% H_2O/10% D_2O) at a protein concentration of 0.5 to 0.8 m*M* for all NMR studies. The sequential backbone resonance assignments of His_6-$XAF1_{214–301}$ and $XIAP^{RING}$ were obtained using two-dimensional $^1H–^{15}N$ HSQC, three-dimensional HNCO, HCACO, HNCACB and HN(CO) CACB spectra. The chemical shift index (CSI) was calculated from the chemical shifts of backbone carbonyl, Cα and Cβ atoms according to Wishart.[32] The CSI values were used to predict the secondary structure.[32]

For titration studies of $XIAP^{RING}$ and $XAF1^{RBD}$, the $XAF1^{RBD}$ binding surfaces on $XIAP^{RING}$ were mapped using the CSP approach. A series of two-dimensional ^{1}H-^{15}N TROSY-HSQC spectra of a ^{15}N-$XIAP^{RING}$ (0.5 m*M*) were recorded as a function of the increasing amount of unlabeled $XAF1^{RBD}$. The NMR titration experiments were performed until the molar ratios of [$XAF1^{RBD}$]/[^{15}N-$XIAP^{RING}$] reached the values of 1: 1.4. Binding event was monitored by changes in the cross-peaks positions of the ^{1}H-^{15}N TROSY-HSQC spectra. These changes of cross-peak chemical shifts were quantified using combined amide CSP calculated as $\Delta\sigma = [(\Delta\sigma_H)^2 + (\Delta\sigma_N/5)^2]^{1/2}$, where $\Delta\sigma_H$ and $\Delta\sigma_N$ are the observed chemical shift changes for ^{1}H and ^{15}N dimensions, respectively. The titration experiment of ^{15}N-His_6-$XAF1_{214\text{-}301}$ with $XIAP^{RING}$ was performed essentially the same as described in the above paragraph. The effects of line broadenings were estimated by measuring the ratios of the intensities for each peak in ^{1}H-^{15}N HSQC spectra, in the absence of $XIAP^{RING}$ and the presence of a 1:1 complex.

References

1. Liston P, Fong WG, Kelly NL, Toji S, Miyazaki T, Conte D, Tamai K, Craig CG, McBurney MW, Korneluk RG (2001) Identification of XAF1 as an antagonist of XIAP anti-caspase activity. Nat Cell Biol 3:128–133.
2. Fong WG, Liston P, Rajcan-Separovic E, St Jean M, Craig C, Korneluk RG (2000) Expression and genetic analysis of XIAP-associated factor 1 (XAF1) in cancer cell lines. Genomics 70:113–122.
3. Ng KC, Campos EI, Martinka M, Li G (2004) XAF1 expression is significantly reduced in human melanoma. J Invest Dermatol 123:1127–1134.
4. Zou B, Chim CS, Zeng H, Leung SY, Yang Y, Tu SP, Lin MC, Wang J, He H, Jiang SH, Sun YW, Yu LF, Yuen ST, Kung HF, Wong BC (2006) Correlation between the single-site CpG methylation and expression silencing of the XAF1 gene in human gastric and colon cancers. Gastroenterology 131:1835–1843.
5. Straszewski-Chavez SL, Visintin IP, Karassina N, Los G, Liston P, Halaban R, Fadiel A, Mor G (2007) XAF1 mediates tumor necrosis factor-alpha-induced apoptosis and X-linked inhibitor of apoptosis cleavage by acting through the mitochondrial pathway. J Biol Chem 282: 13059–13072.
6. Yin W, Cheepala S, Clifford JL (2006) Identification of a novel splice variant of X-linked inhibitor of apoptosis-associated factor 1. Biochem Biophys Res Commun 339:1148–1154.
7. Fang X, Liu Z, Fan Y, Zheng C, Nilson S, Egevad L, Ekman P, Xu D (2006) Switch to full-length of XAF1 mRNA expression in prostate cancer cells by the DNA methylation inhibitor. Int J Cancer 118:2485–2489.
8. Eckelman BP, Salvesen GS, Scott FL (2006) Human inhibitor of apoptosis proteins: why XIAP is the black sheep of the family. EMBO Rep 7:988–994.
9. Tse MK, Hui SK, Yang Y, Yin ST, Hu HY, Zou B, Wong BC, Sze KH (2011) Structural analysis of the UBA domain of X-linked inhibitor of apoptosis protein reveals different surfaces for ubiquitin-binding and self-association. PLoS One 6:e28511.
10. Galban S, Duckett CS (2010) XIAP as a ubiquitin ligase in cellular signaling. Cell Death Differ 17:54–60.
11. Arora V, Cheung HH, Plenchette S, Micali OC, Liston P, Korneluk RG (2007) Degradation of survivin by the X-linked inhibitor of apoptosis (XIAP)-XAF1 complex. J Biol Chem 282:26202–26209.
12. Reibarkh M, Malia TJ, Wagner G (2006) NMR distinction of single- and multiple-mode binding of small-molecule protein ligands. J Am Chem Soc 128:2160–2161.
13. Mace PD, Linke K, Feltham R, Schumacher FR, Smith CA, Vaux DL, Silke J, Day CL (2008) Structures of the cIAP2 RING domain reveal conformational changes associated with ubiquitin-conjugating enzyme (E2) recruitment. J Biol Chem 283:31633–31640.
14. Pickart CM (2001) Mechanisms underlying ubiquitination. Annu Rev Biochem 70:503–533.
15. Plechanovova A, Jaffray EG, McMahon SA, Johnson KA, Navratilova I, Naismith JH, Hay RT (2011) Mechanism of ubiquitylation by dimeric RING ligase RNF4. Nat Struct Mol Biol 18:1052–1059.
16. Hu S, Yang X (2003) Cellular inhibitor of apoptosis 1 and 2 are ubiquitin ligases for the apoptosis inducer Smac/DIABLO. J Biol Chem 278:10055–10060.
17. Leaman DW, Chawla-Sarkar M, Vyas K, Reheman M, Tamai K, Toji S, Borden EC (2002) Identification of X-linked inhibitor of apoptosis-associated factor-1 as an interferon-stimulated gene that augments TRAIL Apo2L-induced apoptosis. J Biol Chem 277: 28504–28511.
18. Suzuki Y, Nakabayashi Y, Takahashi R (2001) Ubiquitin-protein ligase activity of X-linked inhibitor of apoptosis protein promotes proteasomal degradation of caspase-3 and enhances its anti-apoptotic effect in Fas-induced cell death. Proc Natl Acad Sci USA 98:8662–8667.
19. MacFarlane M, Merrison W, Bratton SB, Cohen GM (2002) Proteasome-mediated degradation of Smac during apoptosis: XIAP promotes Smac ubiquitination in vitro. J Biol Chem 277:36611–36616.
20. Shibata T, Noguchi T, Takeno S, Gabbert HE, Ramp U, Kawahara K (2008) Disturbed XIAP and XAF1 expression balance is an independent prognostic factor in gastric adenocarcinomas. Ann Surg Oncol 15:3579–3587.
21. Perrelet D, Perrin FE, Liston P, Korneluk RG, MacKenzie A, Ferrer-Alcon M, Kato AC (2004) Motoneuron resistance to apoptotic cell death in vivo correlates with the ratio between X-linked inhibitor of apoptosis proteins (XIAPs) and its inhibitor, XIAP-associated factor 1. J Neurosci 24:3777–3785.
22. Sun L, Chen ZJ (2004) The novel functions of ubiquitination in signaling. Curr Opin Cell Biol 16:119–126.
23. Mukhopadhyay D, Riezman H (2007) Proteasome-independent functions of ubiquitin in endocytosis and signaling. Science 315:201–205.
24. Di Fiore PP, Polo S, Hofmann K (2003) When ubiquitin meets ubiquitin receptors: a signalling connection. Nat Rev Mol Cell Biol 4:491–497.
25. Tang ED, Wang CY, Xiong Y, Guan KL (2003) A role for NF-kappaB essential modifier/IkappaB kinase-gamma (NEMO/IKKgamma) ubiquitination in the activation of the IkappaB kinase complex by tumor necrosis factor-alpha. J Biol Chem 278:37297–37305.
26. Dynek JN, Goncharov T, Dueber EC, Fedorova AV, Izrael-Tomasevic A, Phu L, Helgason E, Fairbrother WJ, Deshayes K, Kirkpatrick DS, Vucic D (2010) c-IAP1 and UbcH5 promote K11-linked polyubiquitination of RIP1 in TNF signalling. EMBO J 29:4198–4209.
27. Huang H, Joazeiro CA, Bonfoco E, Kamada S, Leverson JD, Hunter T (2000) The inhibitor of apoptosis, cIAP2, functions as a ubiquitin-protein ligase and promotes in

vitro monoubiquitination of caspases 3 and 7. J Biol Chem 275:26661–26664.
28. Vaux DL, Silke J (2005) IAPs, RINGs and ubiquitylation. Nat Rev Mol Cell Biol 6:287–297.
29. Lipkowitz S, Weissman AM (2011) RINGs of good and evil: RING finger ubiquitin ligases at the crossroads of tumour suppression and oncogenesis. Nat Rev Cancer 11:629–643.
30. Wilkinson JC, Wilkinson AS, Galban S, Csomos RA, Duckett CS (2008) Apoptosis-inducing factor is a target for ubiquitination through interaction with XIAP. Mol Cell Biol 28:237–247.
31. Lorick KL, Jensen JP, Weissman AM, Expression, purification, and properties of the Ubc4/5 family of E2 enzymes. In: Raymond JD, Ed. (2005) *Methods in enzymology* Vol. 398. Elsevier Academic Press, San Diego, California, USA, pp 54–68.
32. Wishart DS (2011) Interpreting protein chemical shift data. Prog Nucl Magn Reson Spectrosc 58:62–87.